Flexible organic–inorganic hybrid layer encapsulation for organic opto-electronic devices

Subimal Majee[a,*], Maria Fátima Cerqueira[b], Denis Tondelier[a], Bernard Geffroy[a,c], Yvan Bonnassieuxa, Pedro Alpuim[b,d], Jean Eric Bourée[a]

[a]Laboratoire de Physique des Interfaces et des Couches Minces, Ecole Polytechnique, CNRS UMR 7647, 91128 Palaiseau, France

[b]Centro de Física, Universidade do Minho, 4710-057 Braga, Portugal

[c]Laboratoire de Chimie des Surfaces et Interfaces, IRAMIS/SPCSI CEA Saclay, 91191 Gif-sur-Yvette, France

[d]INL - International Iberian Nanotechnology Laboratory, 4715-330 Braga, Portugal

Keywords:Permeation barrier; Silicon nitride; HW-CVD; PMMA; Organic electronics

Abstract

In this work we produce and study the flexible organic–inorganic hybrid moisture barrier layers for the protection of air sensitive organic opto-electronic devices. The inorganic amorphous silicon nitride layer (SiN_x:H) and the organic PMMA [poly (methyl methacrylate)] layer are deposited alternatingly by using hot wire chemical vapor deposition (HW-CVD) and spin-coating techniques, respectively. The effect of organic–inorganic hybrid interfaces is analyzed for increasing number of interfaces. We produce highly transparent (~80% in the visible region) hybrid structures. The morphological properties are analysed providing a good basis for understanding the variation of the water vapor transmission rate (WVTR) values. A minimum WVTR of 4.5×10^{-5} g/m^{2}day is reported at the ambient atmospheric conditions for 7 organic/inorganic interfaces. The hybrid barriers show superb mechanical flexibility which confirms their high potential for flexible applications.

1. Introduction

Organic opto-electronic devices, such as, organic light emitting diodes (OLEDs) and organic photovoltaic devices (OPVs) are emerging rapidly due to their lower production cost, better mechanical flexibility and lower consumption of materials compared to their inorganic counterparts [1,2]. However, their utilization is limited by the degradation of the devices due to environmental moisture and oxygen. The organic active layers and

the metal electrode used in those devices react with water vapor and oxygen leading to the failure of the complete device. Therefore, the primary challenge before the wide spread commercialization of those products is the development of efficient moisture barrier layers which can protect the active layer and the electrodes from the moisture and oxygen. There is a wide range of permeation barrier requirements for different devices and applications. For the normal food packaging technologies, the encapsulation barrier requirement is not as stringent as for the electronic devices and a single polymer film is sufficient to provide the required efficient packaging. Generally, devices such as OLEDs that use chemically reactive electrodes have the highest sensitivity to moisture, and degradation is observed at the organic layer/electrode interface [3–5]. The extensively used term in the literature to define the steady state permeation of water vapor is water vapor transmission rate (WVTR). WVTR is defined as the amount of water molecules diffusing through a unit area of the barrier film per unit time under conditions of the test and is expressed in g/m^2day. The most widely accepted value for required WVTR for an OLED is in the range of 10^{-6} to $10^{-5} g/m^2day$. This value was originally estimated by calculating the amount of water and oxy-gen needed to degrade the reactive cathode [5]. Other experimental methods also confirmed this value to be a reasonable estimate [6]. The permeation barrier requirements for organic solar cells are determined mainly by the solar cell absorber material that is used. A water vapor transmission rate of $10^{-6} g/m^2day$ was previously reported to avoid degradation of organic solar cells [7]. However, recent studies have shown that for organic solar cells WVTR in the range of 10^{-4} to $10^{-3} g/m^2day$ is quite sufficient to achieve lifetimes of several thousands of hours in operation [8,9].

The existing methods of encapsulation such as hermetic sealing of devices fabricated on glass substrates using a metal or glass lid are not useful for flexible applications. Thin film encapsulation is an attractive solution because of its flexibility and light weight. Recently, almost defect free single-layers of thin films deposited by atomic layer deposition (ALD) showed excellent barrier properties [10–15]. However, the deposition process is slow and the number of materials that can be deposited is limited. On the other hand, the conventional plasma enhanced CVD (PE-CVD) systems used for developing thin film barriers give rise to less dense materials than requested for effective moisture protection [16–19]. Multilayer of thin films is the widely used solutions to hinder the propagation of defects from one layer to the next layer. The organic/inorganic alternating layer structure showed excellent barrier properties for devices fabricated on flexible polymer substrates. The soft organic layer being sandwiched between two consecutive hard inorganic layers decouples the defects from both hard layers, thus avoiding pinhole channeling and absorbs the stresses induced in the hard inorganic layers due to its inherent robustness and high compliance [20–29].

Table 1- Optimized deposition conditions for SiN_x:H films by HW-CVD system.

Parameters	Value
SiH_4 flow rate $F(SiH_4)$ (sccm)	2
NH_3 flow rate $F(NH_3)$ (sccm)	4
H_2 flow rate $F(H_2)$ (sccm)	54
H_2 dilution $(D_H) = F(H_2)/[F(H_2) + F(SiH_4) + F(NH_3)]$	90%
Process gas pressure p_g (mTorr)	25
Nominal substrate temperature T_s (°C)	100
Filament–substrate distance $d_{f\text{-}s}$ (cm)	7.5
Filament temperature T_f (°C)	2000
Electric current supplied to the filament (A)	16
Deposition rate r_d (Å/s)	1.1

In this study, we have deposited inorganic amorphous silicon nitride (SiN_x:H) thin films using hot wire chemical vapor deposition (HW-CVD) to be used as the inorganic part of the hybrid(organic/inorganic) barriers. This deposition technique is advantageous in terms of higher deposition rate (compared to ALD) and higher density films due to lower hydrogen content (compared to PE-CVD). HW-CVD also allows depositing thin films at low substrate temperature which is a major issue for the compatibility with the flexible polymer substrates. Additionally, low substrate damage (due to absence of ion bombardments) during processing and con-formal step coverage allows one to deposit high quality barrier films [30–38]. The quality of the other part of the hybrid barrier structure, i.e. the organic layer is quite important in order to improve the over-all barrier properties. Very recently, several researchers developed high quality organic films with very precise thickness and optical properties. Initiated-CVD (i-CVD) is one of those techniques which could allow one to grow high quality organic layers [28]. Similar to our previous work, we have deposited organic PMMA [poly (methylmethacrylate)] film in between two consecutive inorganic layers using the simple and widely used spin-coating technique [29]. We focus on the effect of organic-inorganic interfaces in reducing the diffusion of water molecules. Several characterizations have been performed in order to interpret the interface effect.

2. Experimental methods

SiN_x:H single-layers have been deposited in this study using HW-CVD. The detailed description of the HW-CVD chamber is given in [36–38]. A single coil shaped Ta filament was resistively heated up to 2000◦C. Silane and ammonia, diluted in hydrogen were used as reactant gases. The gases are pyrolytically decomposed into radical species at the surface of the heated filament, which as a catalyst and provides the precursors for SiN_x:H film growth on the PET substrates. The substrate was kept at a distance of 7.5 cm from the filament and was heated to a temperature of 100◦C in order to stay below the glass transition temperature of the plastic substrates. The substrate temperature was

measured with a thermocouple embedded in the stainless steel substrate-holder, close to the substrate. SiN_x:H single-layers were deposited using the optimized deposition conditions (Table 1) reported previously [37]. In order to avoid the radiation damage of the substrate by the hot filament, the single-layer thickness was kept fixed at 50 nm which is also the critical thickness for permeation as found before [38]. The critical thickness is the single-layer thickness above which there is no more barrier improvement. The critical thickness was used as the inorganic single-layer thickness to fabricate the organic/inorganic hybrid structures.

The above mentioned deposition conditions gave rise to trans-parent (transmittance, T > 80% in the visible region) SiN_x:H thin films. The refractive index (n) of the film was measured using spectroscopic ellipsometry. The value found for the films refractive index (2.01 at 632.8 nm) is close to those found in stoichiometric films [37]. The compositional and structural characterizations of the deposited films were previously reported [36–38].The organic material to be used as the defect-decoupling inter-layer between two inorganic layers should have some intrinsic properties in order to be compatible with the encapsulation pro-cess. The inorganic layers were deposited by HW-CVD in vacuum, and therefore the organic material should be stable during the deposition process. The organic material has low glass transition temperature, which nevertheless should be higher than 100◦C which is the nominal substrate temperature during depositions. Furthermore, they should be stable to the radicals generated in the HW-CVD process.

The organic layer should also have smoothing effect in order to enhance the growth of the next inorganic layer with better structural quality. Additionally, the organic material should have lower Young's modulus (Y) in order to be compliant and flexible [39]. In the present study, PMMA (Y ≈ 3 GPa) was used as an organic material, because it is widely used and inexpensive compared to other organic polymers. The glass transition temperature (T_g) of 106◦C allows it to be stable during the inorganic film deposition. However, the impact of radicals produced inside hotwire CVD chamber on PMMA material has not been investigated in this study.

The organic polymer layer was deposited by spin-coating pro-cess after each SiN_x:H single-layer deposition by HW-CVD. After the SiN_x:H film deposition the sample was transferred to the spin-coater system. The commercially available PMMA was dissolved in chloroform (5 wt.%) and the solution was spin-coated on the already grown SiNx:H film at 4000 rpm for 50 s. The thickness of the polymer layer was kept fixed at 300 nm and the thickness was measured using Dektak 150 profilometer. The polymer layer was annealed at 100◦C when it was transferred again inside the HW-CVD chamber for the next SiN_x:H film deposition. These steps were repeated in order to increase the number of organic/inorganic interfaces. Four different structures have been developed with increasing number of interfaces from 1 to 7 where the interface between the organic PET substrate and the first inorganic SiN_x:H film has been also counted. The hybrid structures are shown in Fig. 1.

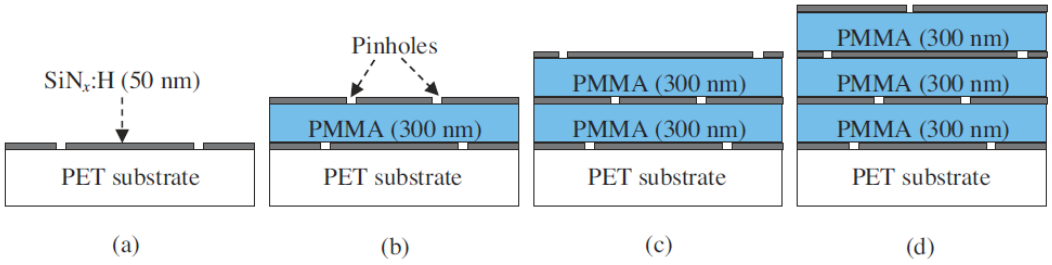

Figure 1- Schematic diagrams of organic/inorganic hybrid structures (not to scale) deposited on PET substrates (175μm): (a) 1 interface, (b) 3 interfaces, (c) 5 interfaces and (d) 7 interfaces.

The surface roughness of the produced hybrid structures was measured using tapping mode atomic force microscopy (AFM) technique. Five different measurements on different positions of the samples have been performed in order to achieve the error value approximation and analyzed using the instrument software. The optical transparency of the hybrid layers was assessed using a Perkin Elmer Spectrophotometer with Integrating Sphere, taking into account the accuracy of the measurement (±1%).

The diffusion barrier properties of the above mentioned hybrid samples have been assessed through electrical calcium degradation test implemented inside the glove box system. The detailed description and schematic diagram of the test setup were reported previously [37, 38]. The Ca thin film (100 nm) and the four Al electrodes (150 nm) were deposited via a thermal evaporator inside the glove box filled with N_2 on the side opposite to the barrier coated PET substrate. Very low deposition rate of 0.2 nm/s at a pressure $<10^{-6}$ mbar was chosen to obtain smooth layers, for both Ca and Al depositions. The whole system was covered with a glass lid using epoxy resin. The water permeation through the epoxy edge-seal is confirmed to be negligible by performing the same test using a glass plate as a reference substrate [37]. Water molecules after diffusing through the whole thickness of the barrier coated substrate reach the Ca sensor and react to form $Ca(OH)_2$ decreasing the conductance of the sensor. The evolution of conductance in time was measured using a four point probe system at the ambient atmosphere. The lag-time of permeation was assessed from the stable region at the beginning of the evolution which is defined as the minimum time taken by the water molecules to diffuse through the whole thickness of the barrier coated substrate to reach the sensor. The WVTR values have been evaluated through the slope of the fitting curve to the conductance curve using the relation:

$$\mathrm{WVTR} = -N\,\delta_{\mathrm{Ca}}\,\rho_{\mathrm{Ca}}\left[\frac{M(\mathrm{water})}{M(\mathrm{Ca})}\right]\cdot\left[\frac{l}{w}\right]\cdot\left[\frac{dG}{dt}\right]\cdot\left[\frac{\mathrm{Area(Ca)}}{\mathrm{Area(window)}}\right]$$

where N is the molar equivalent of the degradation reaction which is assumed as N = 2 from the chemical reaction of Ca with water [$Ca + 2H_2O \rightarrow Ca(OH)2+ H_2$], M is the molar mass of the reactive elements, δ_{Ca} is the density of calcium (1.55 g/cm^3), ρ_{Ca} is the calcium resistivity ($9 \times 10^{-8}\ \Omega$ m), l and ω are the effective length and width of Ca layer respectively and G is the conductance. From the geometry of our setup, the value of Area (Ca)/Area (window) is taken to be unity. It should be noted that sensitivity of the test set-up (10^{-6}g/m^{2}day) was evaluated using a glass substrate and the reproducibility of the set-up was assessed using 20 bare PET substrates which give rise to a WVTR of 0.17 ± 0.05 g/m^{2}day [37].

The actual purpose of the permeation barrier layers is to protect the sensitive devices deposited on plastic substrates for flexible applications. The brittle inorganic materials used as a permeation barrier film for hybrid layer structures have pinholes or defects which arise due to the processing conditions. However, the failure mechanics of the layers depends extensively on their mechanical properties and adhesion to the underlying layer or to the substrate. The mechanical flexibility of the barrier-coated substrates was characterized by bending the structure for several time cycles to a fixed radius of curvature (r). For the bending test, a home-made four-point bending bridge was used and the sample was bent for several load/unload cycles using an automated motor system. The bending of the sample gives rise to tensile strain inside the films, which in turn forms cracks by the formation and/or propagation of interfacial delamination cracks between two consecutive layers [40]. Ca degradation test was performed on deformed samples after release from the bridge, i.e. under no applied strain, in order to verify the possible damage inflicted by the bending on the permeation barrier properties. The mechanical flexibility of the hybrid structure was investigated by bending the hybrid structures with a radius of curvature of 5 mm for different number of cycles of bending.

3. Results and discussion

3.1. Morphological properties

The surface morphology of the as deposited and annealed PMMA films was analyzed by depositing the films on clean corning glass substrates. PMMA becomes smoother when annealed near its glass transition temperature (T_g) of 106◦C [41]. The average surface roughness of the PMMA layer (R_{avg}.= 1.6 nm) decreases ∼80% when it is annealed (R_{avg}.= 0.3 nm) [29]. The change in the morphology at the annealing temperature of around 100◦C is possibly due to intensified thermal diffusions of molecules at the surface of the polymer layer at higher temperatures. The external energy (heat) leads to the minimization of surface energy at the surface of the film which in turn minimizes the effective surface area. Minimization of effective surface area is equivalent to the reduction of surface roughness. Morphological modification of

the PMMA layer helps in hindering the propagation of any structural defects and produces the subsequent inorganic layer with high quality.

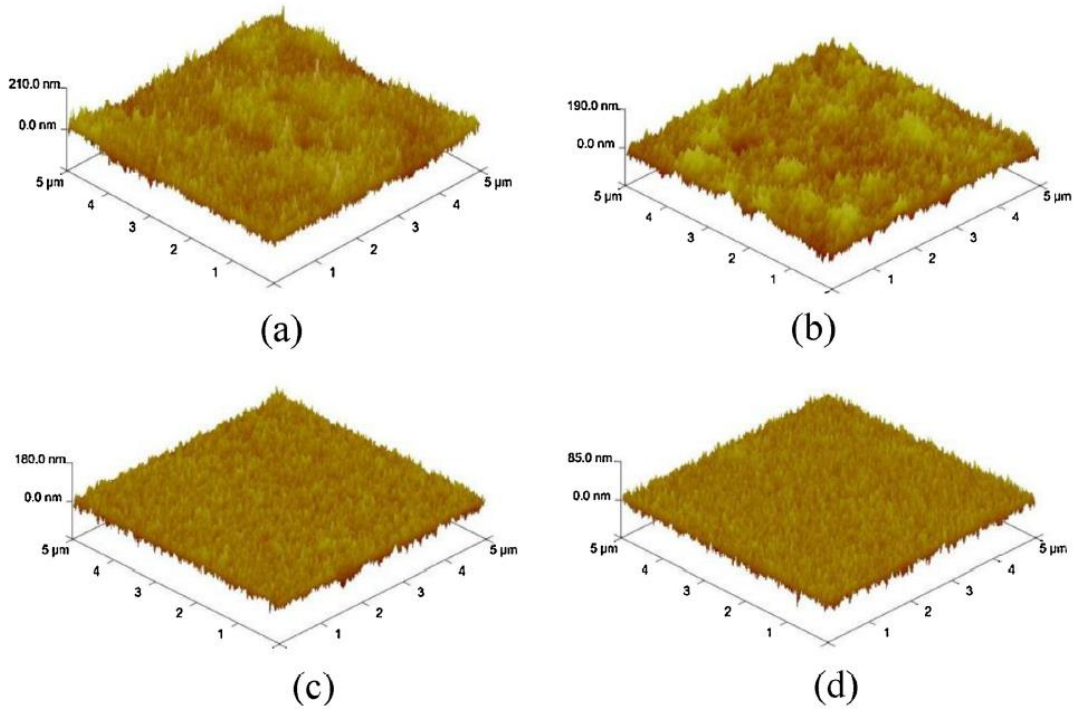

Figure 2 - Three dimensional AFM images of the surfaces of the hybrid structures with increasing number of organic/inorganic interfaces: (a) 1 interface, (b) 3 interfaces, (c) 5 interfaces and (d) 7 interfaces.

Fig. 2 shows the three dimensional surface topographies of the hybrid structures and the variation of average surface roughness values of those structures with increasing number of organic/inorganic interfaces is shown in Fig. 3. The average rough-ness of the bare PET substrate after exposure to the hot filament for the same time (400 s) as it takes for one single-layer (50 nm) deposition, but without film growth, is around 55 nm. The roughness of PET increases strongly from 1.4 nm to 55 nm when the PET foil is exposed to the heated Ta filament, probably due to the fact that the glass transition of PET at around 80◦C is somewhat overcome (100◦C) inducing a warping of the foil. This explains the high initial roughness of the SiN_x:H single-layer film (1 inter-face) deposited on PET substrates. The roughness decreases sharply when the first PMMA layer is inserted between two consecutive SiN_x:H single-layers (3 interfaces) which decreases monotonically with increasing number of organic/inorganic interfaces reaching down to a minimum surface roughness of 7.2 ± 1.5 nm for 7 interfaces. This result shows the planarization effect of PMMA layer which in turn reduces the roughness of the whole structure. It was reported previously that the permeation of the water molecules through the barriers depends largely on the roughness of the layers [38,

42, 43] and it is desired to obtain flat surfaces in order to ease the stacking of successive layers. From this initial result of average roughness reduction, it is expected that the permeation of water molecules will be reduced similarly when the number of organic/inorganic interfaces will be increased.

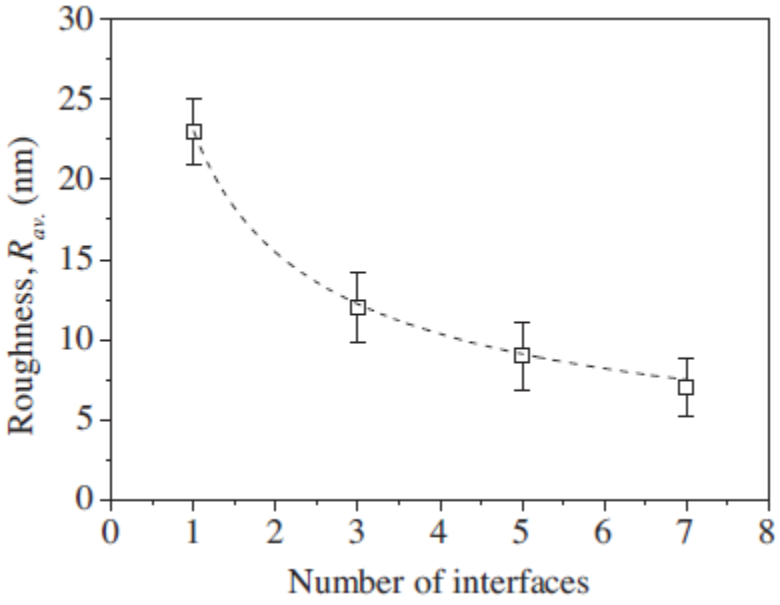

Figure 3 - Variation of average surface roughness with number of organic/inorganic interfaces.

3.2. Optical properties

High optical transparency of the encapsulation barrier film is required for the application to the organic opto-electronic devices. Fig. 4 shows the reflectance (R) and the transmittance (T) measurements of the alternating layer structures. The transmittance curves indicate that all the alternating layer structures are highly transparent (~80%) in the range between 350 and 800 nm. The transmittance is slightly reduced (~5 percentual points) when the number of interfaces is increased from 3 to 7. It can also be seen from Fig. 4 that reflectance and transmittance of this hybrid layer structures together add to almost 100%, meaning that no absorption takes place inside the layers in the visible region and the barrier structures can be perfectly used as window layers for organic opto-electronic devices. Slight absorption below 350 nm wavelength is due to the plastic substrate itself [37].

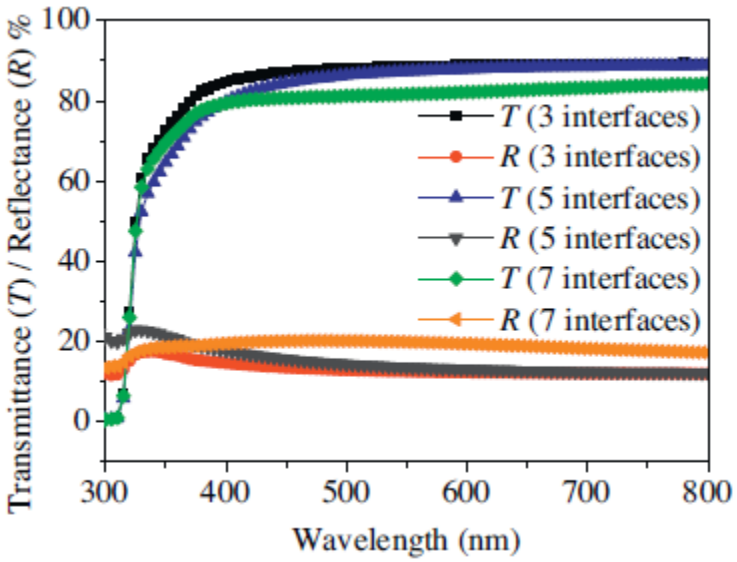

Figure 4- Reflection and transmission spectra of hybrid structures deposited on PET substrates.

3.3. Barrier properties

The evolutions of normalized conductance of the Ca sensors deposited on such hybrid-barrier coated PET substrates are shown in Fig. 5(a). The lag-time and WVTR values are assessed from the evolution of the conductance and are shown in Fig. 5(b). The results show a clear trend of barrier improvement with an increasing number of interfaces, the most dramatic change occurring for an increase from one to three interfaces. The single-layer of SiN_x:H (50 nm) shows no significant reduction of permeation rate. The WVTR value for 50 nm SiN_x:H single-layer is $\sim 10^{-2} g/m^2 day$ which is only one order of magnitude lower than the bare PET substrate(0.17 g/m2day). This value is far beyond the desired permeation rate. When the PMMA layer is inserted between two consecutive SiN_x:H single-layers, the organic layer hinders the native nucleation centres that already existed at the top of the first SiN_x:H layer from propagating into the next layer. When a second SiN_x:H layer is grown on top of the PMMA layer, there is a low probability of alignment of pinholes with the first SiN_x:H layer. Thus the organic interlayer decouples the defects between two successive inorganic layers and makes the diffusion path of water molecules more complex and tortuous. This complex diffusion path makes the total diffusion path of the water molecules longer to reach the calcium sensor which is at the opposite side of the barrier coated PET substrate. This in turn increases the total time of diffusion and the lag-time is increased. The lag-time increases monotonically with increasing number of organic/inorganic interfaces, at least up to 7 interfaces which was the maximum number of inter-faces tested here, and thus with the increase in the total barrier thickness. A maximum lag-time of 155 h is achieved for the 7 inter-faces structure. The WVTR value decreases similarly with variation of average surface roughness (Fig. 3) when the number of interfaces is increased from 1 to 7. As mentioned above, there is a significant drop of WVTR value when the first PMMA layer is inserted between two 50 nm SiN_x:H

single-layers (3 hard/soft interfaces), reaching down to 9.2×10^{-5}g/m^{2}day, confirming the defect-decoupling effect of the smooth PMMA layer. After that WVTR values decreases monotonically with increasing number of interfaces reaching a minimum value of 4.5×10^{-5}g/m^{2}day for 7 interfaces.

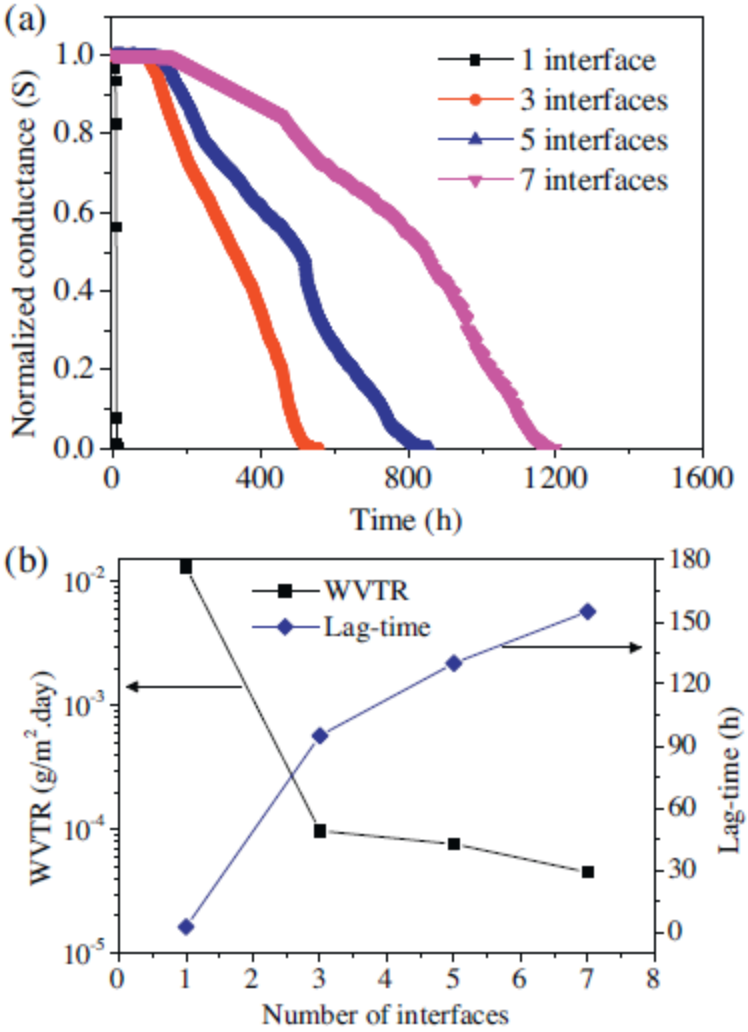

Figure 5 - (a) Evolution of normalized conductance of the Ca sensor with time for different hybrid structures deposited on PET with increasing number of interfaces. (b) Variation of the corresponding lag-time and WVTR with number of interfaces (lines are mere guides to the eye).

3.4. Mechanical properties

Fig. 6 shows the Ca degradation test results after different number of bending cycles performed on the SiN_x:H double-layer without any PMMA layer and SiN_x:H double-layer separated by one PMMA layer (3 interface structure). The barrier properties of the SiN_x:H double-layer without any PMMA layer degrade consider-ably when the number of bending cycles is increased, possibly due to the formation of channel cracks by the deformation. The SiN_x:H double-layer separated by one PMMA layer shows almost no

significant degradation of the barrier properties even after 500 bending cycles. This is probably due to the fact that during deformation, the more compliant under-layer (PMMA) absorbs the stress induced by the bending thus releasing the stress from the inorganic layers and decreases the probability of any crack formation. The observations show that these hybrid structures can keep its moisture barrier properties even if it is bent many times and that the structure can therefore be used for flexible barrier applications.

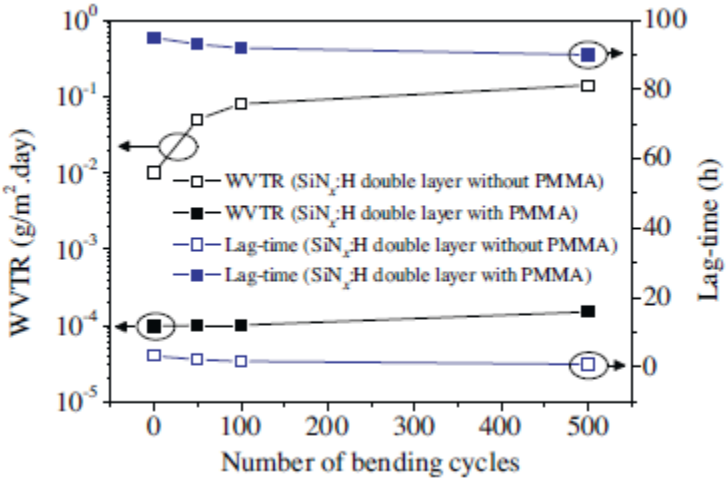

Figure 6 - Variation of lag-time and WVTR with number of bending cycles.

4. Conclusion

In conclusion, we demonstrated excellent permeation barrier properties of organic/inorganic hybrid barrier layers produced by combining HW-CVD technique, for growing inorganic SiN_x:H layer, and simple spin-coating procedure for the organic PMMA polymer layer. The organic layer to improve the quality, we have focussed our attention to realize the effect of organic-inorganic interfaces. The effect of interface is quite critical in order to hinder the nucleation centres of defects at the surface of the inorganic films and thus prevent the alignment of pinholes in the consecutive SiN_x:H layers. Increasing the number of organic/inorganic interfaces, we have obtained an overwhelming reduction of the WVTR value down to4.5×10^{-5}g/m^{2}day and an increase of the lag-time up to 155 hat the ambient atmospheric conditions. This low value of WVTR should be sufficient for extending the shelf-lifetimes of organic devices by protecting them from the moisture and oxygen. The variation of the WVTR values showed a high degree of correlation with the variation of the average surface roughness values and thus qualified the planarization effect of the polymer layer. The hybrid barriers showed excellent transparency (~80%) in the visible region and therefore proved the effectiveness in the utilization for flexible organic opto-electronic devices. The barrier structure also showed superb flexibility even after 500 bending cycles which allows for flexible barrier applications. Further development of the barrier structures can be obtained by improving the structural quality of the organic interlayers.

Acknowledgments

The authors would like to thank Dr. J.C. Vanel for help in electrical characterizations used in this study. The first author (S.M) acknowledges the financial support from Direction des Relations Extérieures, Ecole Polytechnique during his thesis.

References

[1] N. Grossiord, J.M. Kroon, R. Andriessen, P.W.M. Blom, Org. Electron. 13 (2012) 432.

[2] C.J. Brabec, J.A. Hauch, P. Schilinsky, C. Waldauf, MRS Bull. 30 (2005) 50.

[3] J. Lewis, Mater. Today 9 (2006) 4.

[4] F. Papadimitrakopoulos, X.M. Zhang, K.A. Higginson, IEEE J. Sel. Top. Quant. Electron. 4 (1998) 1.

[5] P.E. Burrows, G.L. Graff, M.E. Gross, P.M. Martin, M. Hall, E. Mast, C.C. Bonham,W.D. Bennett, L.A. Michalski, M.S. Weaver, J.J. Brown, D. Fogarty, L.S. Sapochak,Proc. SPIE 4105 (2001) 75.

[6] M.S. Weaver, L.A. Michalski, K. Rajan, M.A. Rothman, J.A. Silvernail, J.J. Brown, P.E. Burrows, G.L. Graff, M.E. Gross, P.M. Martin, M. Hall, E. Mast, C. Bonham, W.Bennett, M. Zumhoff, Appl. Phys. Lett. 81 (2002) 2929.

[7] G. Dennler, C. Lungenschmied, H. Neugebauer, N.S. Sariciftci, M. Latrèche, G.Czeremuszkin, M.R. Wertheimer, Thin Solid Films 511–512 (2006) 349.

[8] J.A. Hauch, P. Schilinsky, S.A. Choulis, S. Rajoelson, C. Brabec, J. Appl. Phys. Lett.93 (2008) 103306.

[9] S. Cros, R. de Bettignies, S. Berson, S. Bailly, P. Maisse, N. Lemaitre, S. Guillerez,Sol. Energy Mater. Sol. Cells 95 (2011) S65.

[10] P.F. Carcia, R.S. McLean, M.H. Reilly, M.D. Groner, S.M. George, Appl. Phys. Lett.89 (2006) 031915.

[11] S.H.K. Park, J. Oh, C.S. Hwang, J.I. Lee, Y.S. Yang, H.Y. Chu, K.Y. Kang, ETRI J. 27(2005) 545.

[12] W.J. Potscavage, S. Yoo, B. Domercq, B. Kippelen, Appl. Phys. Lett. 90 (2007) 253511.

[13] A.P. Ghosh, L.J. Gerenser, C.M. Jarman, J.E. Fornalik, Appl. Phys. Lett. 86 (2005) 223503.

[14] Y.Q. Yang, Y. Duan, P. Chen, F.B. Sun, Y.H. Duan, X. Wang, D. Yang, J. Phys. Chem.C 117 (39) (2013) 20308.

[15] S.W. Seo, E. Jung, C. Lim, H. Chae, S.M. Cho, Appl. Phys. Exp. 5 (2012) 035701.

[16] Y. Leterrier, Prog. Mater. Sci. 48 (2003) 1.

[17] A.S. da Silva Sobrinho, M. Latrèche, G. Czeremuszkin, J.E. Klemberg-Sapieha,M.R. Wertheimer, J. Vac. Sci. Technol. A 16 (1998) 3190.

[18] W. Huang, X. Wang, M. Sheng, L. Xu, F. Stubhan, L. Luo, T. Feng, X. Wang, F.Zhang, S. Zou, Mater. Sci. Eng.: B 98 (2003) 248.

[19] P. Mandlik, J. Gartside, L. Han, I.C. Cheng, S. Wagner, J.A. Silvernail, R.Q. Ma, M.Hack, J. Brown, J. Appl. Phys. Lett. 92 (2008) 103309.

[20] G. Nisato, M. Kuilder, P. Bouten, Proc. Soc. Inform. Display Symp. Dig. Tech.Papers 34 (2003) 550.

[21] T.N. Chen, D.S. Wuu, C.C. Wu, C.C. Chiang, Y.P. Chen, R.H. Horng, Plasma Process.Polym. 4 (2007) 180.

[22] A.B. Chwang, M.A. Rothman, S.Y. Mao, R.H. Hewitt, M.S. Weaver, J.A. Silvernail,K. Rajan, M. Hack, J.J. Brown, X. Chu, L. Moro, T. Krajewski, N. Rutherford, Appl.Phys. Lett. 83 (2003) 413.

[23] T.W. Kim, M. Yan, A.G. Erlat, P.A. McConnelee, M. Pellow, J. Deluca, T.P. Feist,A.R. Duggal, M. Schaepkens, J. Vac. Sci. Technol. A 23 (2005) 971.

[24] M. Yan, T. Wonkim, A.G. Erlat, M. Pellow, D.F. Foust, J. Liu, M. Schaepkens,C.M. Heller, P.A. McConnelee, T.P. Feist, A.R. Duggal, Proc. IEEE 93 (2005) 1468.

[25] K. Akedo, A. Miura, H. Fujikawa, Y. Taga, Proc. Soc. Inform. Display Symp., Dig.Tech. Papers 34 (2003) 559.

[26] C. Lungenschmied, G. Dennler, H. Neugebauer, S.N. Sariciftci, M. Glatthaar, T.Meyer, A. Meyer, Sol. Energy Mater. Sol. Cells 91 (2007) 379.

[27] A. Yoshida, A. Sugimoto, T. Miyadera, S. Miyaguchi, J. Photopolymer Sci. Technol.14 (2001) 327.

[28] D. Spee, K. van der Werf, J. Rath, R. Schropp, Phys. Status Solidi: Rapid Res. Lett.6 (2012) 151.

[29] S. Majee, B. Geffroy, Y. Bonnassieux, J.E. Bourée, Surf. Coat. Technol. 254 (2014) 429.

[30] H. Matsumura, J. Appl. Phys. 66 (1989) 3612.

[31] H. Matsumura, H. Umemoto, A. Izumi, A. Masuda, Thin Solid Films 430 (2003) 7.

[32] A. Masuda, M. Totsuka, T. Oku, R. Hattori, H. Matsumura, Vacuum 74 (2004) 525.

[33] A. Heya, T. Niki, Y. Yonezawa, T. Minamikawa, S. Muroi, A. Izumi, A. Masuda, H.Umemoto, H. Matsumura, Jpn. J. Appl. Phys. 43 (2004) L1362.

[34] Y. Ogawa, K. Ohdaira, T. Oyaidu, H. Matsumura, Thin Solid Films 516 (2008)611.

[35] A. Heya, T. Minamikawa, T. Niki, S. Minami, A. Masuda, H. Umemoto, N. Matsuo,H. Matsumura, Thin Solid Films 516 (5) (2008) 553.

[36] P. Alpuim, L.M. Gonc¸alves, E.S. Marins, T.M.R. Viseu, S. Ferdov, J.E. Bourée, ThinSolid Films 517 (2009) 3503.

[37] S. Majee, M.F. Cerqueira, D. Tondelier, B. Geffroy, Y. Bonnassieux, P. Alpuim, J.E.Bourée, Surf. Coat. Technol. 235 (2013) 361.

[38] S. Majee, M.F. Cerqueira, D. Tondelier, B. Geffroy, Y. Bonnassieux, P. Alpuim, J.E.Bourée, Jpn. J. Appl. Phys. 53 (2014), 05FM05.

[39] Z. Suo, E.Y. Ma, H. Gleskova, S. Wagner, Appl. Phys. Lett. 74 (1999) 1177.

[40] Z. Jia, M.B. Tucker, T. Li, Compos. Sci. Technol. 71 (2011) 365.

[41] M. Na, S.W. Rhee, Org. Electron. 7 (2006) 205.

[42] A.G. Erlat, R.J. Spontak, R.P. Clarke, T.C. Robinson, P.D. Haaland, Y. Tropsha, N.G.Harvey, E.A. Vogler, J. Phys. Chem. B 103 (1999) 6047.

[43] J.D. Affinito, S. Eufinger, M.E. Gross, G.L. Graff, P.M. Martin, Thin Solid Films308–309 (1997) 19.